Available online at www.sciencedirect.com
SCIENCE DIRECT®
International Journal of Mass Spectrometry 226 (2003) 239–248
International Journal of Mass Spectrometry
www.elsevier.com/locate/ijms

The initial-ion velocity as a marker for different desorption-ionization mechanisms in MALDI

Michael Karas*, Ute Bahr, Isabelle Fournier[1], Matthias Glückmann[2], Anja Pfenninger[3]

Institute for Pharmaceutical Chemistry, Johann Wolfgang Goethe-University of Frankfurt, Biocenter, Marie-Curie-Str. 9-11, D-60439 Frankfurt, Germany

Received 4 July 2002; accepted 10 October 2002

Abstract

While the high, mass-independent and matrix-determined initial velocity of matrix-assisted laser desorption ionization (MALDI) ions has been proposed to be a meaningful characteristic feature of the MALDI process and indicative for the generation of a jet of clusters, considerably lower values as obtained for some low-mass non-protein analytes and certain preparation protocols pointed to a possible second and different process of ion generation. In this paper it is shown that only low-mass neutral compounds can be ionized exhibiting initial velocities considerably lower than that determined by the matrix. New results presented in this paper show that there is a gradual increase of the initial velocities with increasing mass for neutral oligosaccharides and technical polymers to the high level characteristic for peptides and proteins which is also obtained for a small oligosaccharide by introduction of a charged functional group via derivatization. This indicates that typical MALDI analytes need incorporation and cluster generation to be detected whereas an evaporation and gas-phase cationization is viable for small neutral analytes. The directionality of the emission of ions is investigated for different preparation protocols and crystallization states of the matrix. In a further experiment, the correlation between a high initial velocity and the softness of the MALDI ion generation is substantiated.

Keywords: MALDI mechanism; Initial ion velocity; Incorporation; Cluster generation

1. Introduction

In a series of experiments, the fundamental mechanisms active in matrix-assisted laser desorption ionization (MALDI) have been readdressed in recent years to overcome apparent limitations of the models discussed. In a first set of experiments the initial velocity of the MALDI ions has been thoroughly investigated and it was concluded that it is a superior tool to characterize the "desorption step" of the MALDI process [1,2]. The matrix-dependent, but analyte mass-independent high initial ion velocity well agrees with the qualitative picture of a jet-like expansion of matrix molecules entraining analyte molecules [3,4]. While this suggests a quasi-instantaneous phase transition from the solid to a (high-pressure) gaseous state, some observations but most importantly elaborate

* Corresponding author. Tel.: +49-69-798-29916; fax: +49-69-798-29918.
E-mail address: karas@iachem.de (M. Karas).
[1] Present address: Université des Sciences et Technologies de Lille, Villeneuve d'Ascq, France.
[2] Present address: Applied Biosystems, Weiterstadt, Germany.
[3] Present address: Aventis Pharma Deutschland GmbH, Frankfurt, Germany.

1387-3806/02/$ – see front matter
PII S1387-3806(02)01062-X

numerical simulations by Zhigilei et al. [5] and Zhigilei and Garrison [6] point to the intermediate occurrence of particulate matter (clusters) as opposed to a uniform process of fluence-dependent and continuously increasing evaporation: while evaporation starts at considerably lower fluences, an explosive ablation into clusters is determined above a certain threshold fluence. This, moreover, delivered the rationale for a new approach to ion formation in MALDI which defines formation of charged clusters as an essential and typical primary "ionization" mechanism in MALDI [7].

The initial ion velocity is well suited to replace the laser fluence as the characteristic measure for the MALDI process. To a first view this is contradictory to the general experience that the applied laser fluence appeared to be so critical, especially in the early MALDI experiments using continuos-extraction time-of-flight (TOF) mass analysis; good results could only be obtained at and near threshold (i.e., low) fluence. However, the widely varying numbers found in the literature presumably based on different experimental set-ups and especially on varying focusing conditions [8–15] casted strong doubts on the meaningfulness of the laser fluence and on the energy-per-volume data deduced from those measurements. With the advent of "delayed ion extraction" some decoupling between ion generation and TOF detection occurred which is complete for MALDI at intermediate pressure in orthogonal TOF systems; again, working at higher laser fluences became possible. Would the laser fluence directly translate into energy-per-volume and into internal energy of the generated ions, the influence of the applied laser fluence would be very strong; it is obvious today that the detrimental (or desired fragmentation-promoting) effects of higher laser fluence are rather due to secondary effects, especially ion–neutral collisions within the acceleration phase of the ions. Within the useful laser fluence range and thus at considerably higher than threshold values the initial ion velocity stays constant proving again the usefulness of this physical value [2]. Since the higher energy density in the uppermost matrix–analyte layer at higher laser fluence does not scale with an increased ion excitation and fragmentation, it appears reasonable to assume that the higher amount of incident laser energy simply results in the ablation of more material and that a very effective cooling mechanism is active [16–18].

As pointed out, the initial velocity proved to be very useful to differentiate matrices and preparation protocols, such as solvent and additives, but most of the initial experiments focused on peptides and proteins. It was, however, already reported that small oligosaccharides exhibited a considerably lower initial velocity [2]. This, together with different preparation protocols applied and their detection as sodiated ion species, pointed to differences in their desorption ionization compared to peptides and proteins. It was, moreover, detected that these small oligosaccharides could be also detected with high quality without a distinct incorporation step, i.e., from pressed solid powder, in strong contrast to peptides and proteins, for which this "preparation" yielded only very inferior results [19].

While the practical importance of the matrix-dependent initial ion velocity is obvious due to its influence on mass calibration in delayed-extraction TOF mass analyzers, this report focuses on its implications for the MALDI process. It will be shown that for most of the MALDI applications a true incorporation and a high initial ion velocity is observed, if high-quality analyte MALDI mass spectra are obtainable; only for low molecular-weight and non-charged compounds low initial velocities are observed pointing to a reduced role of the matrix. Moreover, different preparation protocols are inspected with regard to their influence on the initial ion velocity. It will be shown that the ratio between the normal average ion velocity and that determined under a certain angle is strongly affected by the microscopic characteristics of the sample.

2. Methods and instrumentation

The measurements were performed using two MALDI-TOF mass spectrometers (Voyager DE-PRO

and Voyager DE, Applied Biosystems, Framingham, MA) in the linear mode. Both TOF systems comprise a gridded two-stage ion source (for detailed experimental parameters see below). A newly designed target holder with an additional grid at the level of the regular target and a lowered sample support makes it possible to vary the surface angle towards the normal of the TOF axis and generates a nearly field-free region. Samples were used as commercially supplied. Peptide and matrix samples were obtained from Sigma, Deisenhofen, Germany. Single crystals of analytes and 2,5-dihydroxybenzoic (DHB) acid were produced using saturated matrix solution with 0.1 mM analyte solution (0.1% TFA/water, acetonitrile 2:1 (ATW), 4 °C, 12 h). For the standard dried-droplet preparation, samples were prepared by applying 1 μL of matrix solution (DHB 10 mg/mL ATW, ferulic acid 8 mg/mL ATW) plus 1 μL of analyte solution in ATW. For surface preparation 1 μL of matrix solution (4-hydroxy-α-cyanocinnamic acid (HCCA), 8 mg/mL in acetone) was dried before adding 1 μL of analyte solution to the crystalline matrix surface. Analyte concentration was between 1×10^{-5} and 5×10^{-6} M.

For amination the oligosaccharide was reacted with saturated aqueous NH_4HCO_3 for 6 days at 30 °C; the reaction mixture was diluted with 0.1% TFA and concentrated in vacuo repeatedly for seven times.

For measurement of v_0 as a function of the target-to-TOF axis a modified sample holder was used which made the alignment of the MALDI sample at a variable angle possible.

3. Measurement of the initial ion velocity

Summing up the contributions of the flight-time within the two-stage ion source and the field-free drift-length: $t = t_1 + t_2 + t_3$ the equation for t for the linear TOF is given by

$$t = \frac{\sqrt{2m}}{z}\left[\frac{\sqrt{E_{\mathrm{kin}1}}}{U_1}d_1 - \frac{\sqrt{E_{\mathrm{kin}0}}}{U_1}d_1 + \frac{\sqrt{E_{\mathrm{kin}2}}}{U_2}d_2 - \frac{\sqrt{E_{\mathrm{kin}1}}}{U_2}d_2\right] + L\sqrt{\frac{m}{2E_{\mathrm{kin}2}}}$$

With expansion of the kinetic energies:

$$E_{\mathrm{kin}\,x} = E_{\mathrm{kin}(x/0)} + \frac{v_0}{1!}\frac{\delta E_{\mathrm{kin}(x/0)}}{\delta v_0} + \cdots \qquad (x = 0, 1, 2)$$

results:

$$t = \sqrt{\frac{m}{2zU}}\left[\frac{2d_1}{\sqrt{(1-G)}} - \frac{\tau v_0}{2d_1}\frac{2d_1}{\sqrt{(1-G)}} + \frac{2d_2}{1+\sqrt{(1-G)}} + \frac{\tau v_0}{2d_1}\frac{\sqrt{(1-G)}2d_2}{1+\sqrt{(1-G)}}\right] + (1-G)L\sqrt{\frac{m}{2zU}}\frac{\tau v_0}{2d_1} + L\sqrt{\frac{m}{2zU}}$$

With

$$L_{\mathrm{e}} = \frac{2d_1}{\sqrt{(1-G)}} + \frac{2d_2}{1+\sqrt{(1-G)}} + L$$

and

$$h = (1-G)L - \frac{2d_1}{\sqrt{(1-G)}} + \frac{\sqrt{(1-G)}2d_2}{1+\sqrt{(1-G)}}$$

t can be expressed by

$$t = \sqrt{\frac{m}{2zU}}\left[h\frac{\tau v_0}{2d_1} + L_{\mathrm{e}}\right] \qquad (1)$$

where t (s): time-of-flight, m (kg): ion mass, charge number: z, τ (s): delay-time, E_1 and E_2 (V/m): field strength within the ion source, d_1 and d_2 (m): acceleration gaps 1 and 2, L_{e} (m): field-free drift-length, v_0 (m/s): initial axial ion velocity, U (V): total applied acceleration voltage, and G relative acceleration voltage: $(U - U_1)100/U$.

The time-of-flight is a linear function of τ and v_0 to good approximation. Total flight times t for the ion of interest are measured as a function of τ between 200 and 1200 ns, with 200 ns forming an instrumental minimal delay time; therefore, it has no influence on the measurement (and it cannot be investigated) if the final ions are formed with some time delay as long as these processes are finalized when the extraction voltage is switched on; v_0 is determined from the slope of the linear curve via a numerical fit [2] for known TOF-parameters L, d_1, d_2 (which are $d_1 = 2.43$ mm, $d_2 = 17.4$ mm and $L = 1281.5$ mm,

Table 1
Numerically simulated slopes of t vs. τ for $[\text{insulin} + \text{H}]^+$, $U = 25\,\text{kV}$, $G = 92\%$ (Voyager DE PRO, Applied Biosystems, Framingham, MA)

Experimental slope t_{ges} vs. τ (ns/ns)	Initial velocity v_0 (m/s)
0.2	301
0.3	450
0.4	598
0.5	746
0.6	893

$U = 20{,}000\,\text{V}$, $G = 92\%$, and ion mass m). Since the delayed-extraction TOF resolution is only optimal for one value of τ and a large τ range is inspected, flight times are determined by peak centroiding. As shown in Table 1, differences in the slope of 0.1 ns/ns for $[\text{insulin} + \text{H}]^+$ result in differences of about 100 m/s in v_0.

Even though the relative differences between the different matrices, preparation protocols and ion species would be highly meaningful already, the measurement of the initial velocity of metal cation species directly from the metal target, which yielded a very low value close to "0", indicated that field penetration and thus distorting effects are negligible in the instrument used. This is also true for the second instrument used, within the experimental error the same values are obtained.

4. Results and discussion

4.1. The initial velocity as a tool to control analyte incorporation and to differentiate various desorption-ionization mechanisms

The first set of experiments showed that the initial axial ion velocity is essentially determined by the matrix. Neither ion mass, charge state, ion polarity nor laser fluence showed any significant influence when staying within the analyte class of peptide and proteins [1,2] and within an analytically useful fluence range. The original observation of a wavelength influence [1] was based on a low number of experiments and could not be substantiated in [2]. For DHB large single crystals yielded the same initial velocity as the extended needles formed in the rim within the dried-droplet protocols. Major deviations from these matrix-defined mean values were found for varying preparation protocols, i.e., different solvents or additives which showed deviations to larger or smaller v_0 values, and for small oligosaccharides. For the latter typically DHB is used as a matrix, but the measurement is carried out from the microcrystalline inner droplet area and here a significantly lower initial velocity is determined [2] as compared to the coarse-crystalline outer rim. This prompted further investigations into the role of incorporation within the preparation step [19]: it was found that small oligosaccharides in contrast to peptides and proteins yielded equally good results also from physically mixed particulate material (analyte and matrix) exhibiting again a low initial velocity. It was concluded that a high initial velocity is only observed when analytes are truly incorporated into the matrix host crystals and that this is required for typical peptides (except some cases such as gramicidin S) and proteins, but not for small oligosaccharides (and other thermally stable low-molecular weight compounds).

To further address this separation into different desorption-ionization regimes the following analytes were investigated: two neutral-oligosaccharide oligomer distributions (maltodextrin and human-milk oligosaccharides), polyamide oligomers, an acidic oligosaccharide, an oligosaccharide chemically derivatized to contain a basic functional group and a set of larger neutral oligosaccharides both directly and after permethylation. In all cases DHB was used as the matrix applying a dried-droplet protocol (polyamides and acidic sugars) or an optimized oligosaccharide protocol resulting in a uniform matrix–analyte deposit [20].

The most striking result for the oligomer distributions is that in all cases a clear dependence of the initial ion velocity of the analyte mass is detected. While the low initial velocities are confirmed for small oligosaccharides, a steep rise of the initial velocity is obtained in the mass range between 500 and 1500 Da (see Fig. 1 and Table 2). All compounds, i.e.,

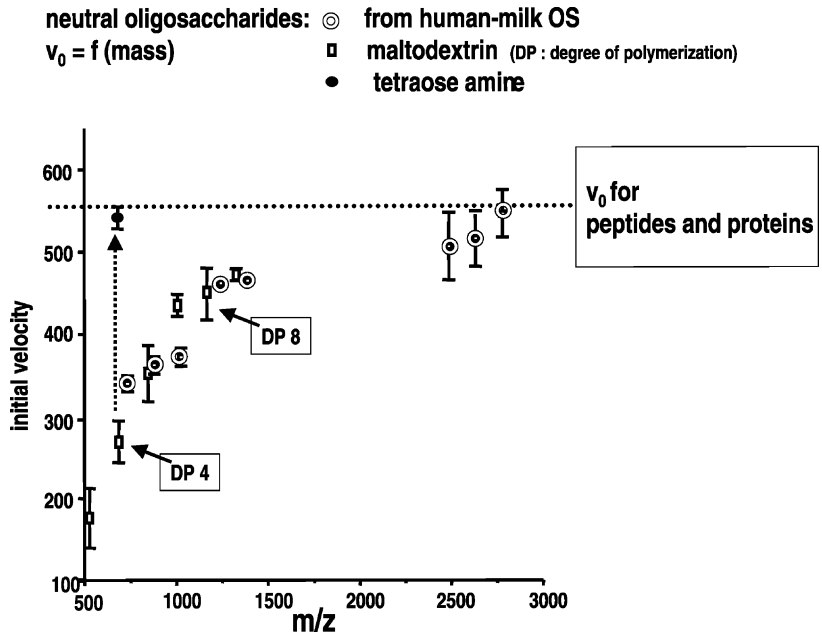

Fig. 1. Comparison of the mass-dependent initial velocities of different oligosaccharides with the (mass-independent) initial velocity obtained for peptides and proteins.

maltodextrin, the neutral human-milk oligosaccharides and the polyamides reach the typical "peptide/protein" velocity at about 2500–3000 Da. Chemical derivatization to a glucoseamin tetraose resulted in the immediate increase of v_0 to the high peptide/protein values (dashed arrow in Fig. 1). Also the acidic oligosaccharide (disialo-lacto-*N*-tetraose (DSLNT)) yielded the high initial velocity and a uniform one for all the different ion species detectable (see Table 3), whereas the initial velocity for a set of three larger human-milk oligosaccharides was significantly reduced by their permethylation (despite the resulting increase in mass) (see Table 4).

These data can be rationalized by a simple approach: the high initial v_0 is a clear indication for a true and soft MALDI process based on the incorporation

Table 2
Initial velocities of a polyamide distribution detected as $[M+Na]^+$ and $[M+H]^+$ (HO–$[CO–(CH_2)_{11}–NH]_n$–CO–$(CH_2)_4$–COOH with n = 2–11, prepared with 10 g/L 2,5-dihydroxybenzoic acid in tetrahydrofuran)

M (g/mol)	v_0 $[M + Na]^+$	v_0 $[M + H]^+$
540	410	393
737	366	390
934	416	423
1131	488	490
1328	513	517
1525	535	530
1722	548	519
1919	548	527
2116	567	566
2313	593	574

Table 3
Initial velocities determined for different ions of an acidic oligosaccharide (disialo-lacto-*N*-tetraose, molecular mass: 1290.2 Da)

Mode	v_0
Positive ion mode	
$[M + Na]^+$	515 ± 14
$[M - H + 2Na]^+$	556 ± 12
$[M - 2H + 3Na]^+$	573 ± 7
Negative ion mode	
$[M - H]^-$	544 ± 29
$[M - 2H + Na]^-$	553 ± 30

Table 4
Comparison of initial velocities for underivatized and permethylated oligosaccharides of the same composition using the same preparation protocol

Composition	Underivatized		Permethylated	
	M (g/mol)	v_0 (m/s)	M (g/mol)	v_0 (m/s)
$[L5/2 - 0 + Na]^+$	2484	506 ± 41	3073	393 ± 2
[L5/3 − 0 + Na]	2630	515 ± 33	3247	416 ± 12
[L5/4 − 0 + Na]	2776	545 ± 29	3421	421 ± 4

1:1 mixture of 2,5-dihydroxybenzoic (DHB) acid, 10 g/L in water/methanol (1:1) and 5 mM NaCl in water; oligosaccharide composition LX/Y − Z: L: lactose, X: number of N-acetyllactose units; Y: number of fucoses, Z: number of sialic acids.

of the analyte. Only small non-charged compounds, such as small sugar oligomers or technical polymers, can be equally well desorbed from a preparation (or areas within a dried-droplet deposit) where only a close contact between analyte and matrix exists. Their desorption ionization is well described as an evaporation followed by gas-phase cationization and the function of the matrix is reduced to facilitate energy deposition and to provide cations in the dense gaseous plume. This evaporative desorption ionization fails even for small charged compounds, such as aminated sugars or acidic sugars, pointing to the fact that these (pre)charged compounds cannot be evaporated without destruction. In a recent paper, using pH-indicator dyes as molecular probes, clear evidence was reported that the charge state of the analyte from solution is roughly preserved in the matrix crystals [21]. In contrast to this evaporative desorption ionization, the incorporation into the matrix crystals, indicated by the uniform, high and matrix-determined initial v_0, enables for a soft and true MALDI process, which is also required for larger neutral compounds. The transition and rise in v_0 is therefore understood as the gradual reduction of the low-velocity "evaporative" component. The high initial v_0 for charged analytes points to the fact that those cationized species are not formed by gas phase ion–neutral reactions, but rather by the generation of charged clusters (cluster ionization) [7].

With regard to the MALDI process, this evaporative desorption ionization does not form an additional general mechanism, but rather a transition from thermal evaporation (without a matrix) by laser heating of the sample and/or metal substrate to an intermediate state where some matrix "support" is active. This is, however, only sufficient and successful for small to medium-size thermally stable neutral analyte compounds and not for large biomolecules accessible by MALDI. One direct practical aspect are calibration problems within a series of oligomers which are indeed observed and well explained by this variation in v_0.

It has to be mentioned that recently a new solvent-free preparation protocol has been published [22] which focused to MALDI applications to technical polymers, but also yielded protein mass spectra. These authors are following a different protocol than used for the experiments reported here and generate an ultrafine powder. The apparent discrepancies can actually not be explained here, possibly moisture from air forms a liquid layer on the very large surface of the ultrafine powder and enhances matrix–analyte interaction. To measure v_0 from these matrix–analyte deposits would be the next step.

4.2. What affects the initial velocity for one matrix compound—solvent, additives and crystalline state

The above clarifications on the analyte role raise the question which matrix properties determine v_0 and how v_0 can be changed. From the existing data it can be concluded that these are parameters which affect the crystal state of the matrix, such as the choice of solvent and additives.

While the first two effects are clearly evident, but not predictable and can result both in a decrease or increase of v_0 [2], experiments on the influence of the microscopic state will be reported in the following. In addition to the axial initial velocity, the angular distribution of v_0 was also inspected by investigating v_0 as a function of the angle between target and TOF axis or by determining the ratio between normal v_0 and that obtained for a 45° tilted sample surface.

DHB was used as the test matrix, since single or large crystals are easily produced, supplemented

Table 5a
Initial velocities obtained for cytochrome *c* for different angles relative to the TOF axis (Voyager DE PRO, Applied Biosystems, Framingham, MA)

Matrix	Ion	v_0 (m/s)	ϑ to TOF-axis (°)	n[a]
DHB, single crystal	Cytochrome *c*	562 ± 97	0	–
DHB, single crystal	Cytochrome *c*	415 ± 104	15	
DHB, single crystal	Cytochrome *c*	359 ± 26	30	
DHB, single crystal	Cytochrome *c*	231 ± 101	40	2.96

[a] Exponent of $\cos\vartheta$.

by HCCA and both coarsely crystalline (rim of dried-droplet preparation) and homogeneous polycrystalline deposits were investigated. For a large crystal doped with cytochrome *c*, the initial velocity of cCH^+ determined as a function of the emission angle showed the profile exhibited in Table 5a. Even though this is not the number distribution of ions emitted as a function of angle, the directionality of the ion emission is also obvious. The dependence of v_0 on the angle is mathematically close to $\cos^2$. Table 5b summarizes the results for the comparative experiments. It is well obvious that the directionality is much more pronounced in the case of large or single crystals which is expressed by the larger ratio between the normal initial velocity and that of 45 (40) degrees. In all cases a slight but significant increase of the axial initial velocity was observed when recording single crystals. While these effects are mass independent up to cytochrome *c*, carbonic anhydrase yields a high initial velocity also at 40°. This v_0 value, however, cannot be regarded as a measure for the forward peaking of the plume. Actually a strong forward peaking has been reported when comparing matrix and analyte ions [23] and has been predicted.

These results substantiate the idea that MALDI desorption is a process essentially controlled by solid/crystal mechanical properties. The better the mechanical confinement, the higher is the initial axial velocity and the ratio between axial and angular v_0. Since the disintegration will proceed normal to the crystal surface independent of the incident angle of the laser, a large closed surface will result in a more directed jet of clusters compared especially to the open surfaces of many tiny crystals where the expansion will be more isotropic into the 2π half sphere, and only the normal component of the initial velocity

Table 5b
Initial velocities obtained for different analyte ions, preparation procedures and angles relative to the TOF axis (Voyager DE PRO, Applied Biosystems, Framingham, MA)

Matrix	Ion	v_0 (m/s)	ϑ to TOF-axis (°)	n[a]
DHB, single crystal	Insulin	551 ± 22	0	
DHB, dried-droplet rim	Insulin	543 ± 40	0	
DHB, surface preparation	Insulin	505 ± 80	0	
DHB, single crystal	Insulin	228 ± 99	45	2.31
DHB, dried-droplet rim	Insulin	362 ± 107	45	0.98
DHB, surface preparation	Insulin	388 ± 56	45	
DHB, dried-droplet	Leu-enkephaline	216 ± 61	45	2.47
DHB, single crystal	Carbonic anhydrase	517	40	0.04
DHB, single crystal	Carbonic anhydrase	502 ± 180	40	0.11
HCCA, single crystal	Insulin	323 ± 39	0	
HCCA, surface preparation	Insulin	290 ± 51	0	
HCCA, single crystal	Insulin	238 ± 57	40	
HCCA, surface preparation	Insulin	285 ± 49	40	

[a] Exponent of $\cos\vartheta$.

shows up in the measurements as the average axial velocity. Moreover, this also explains why optimal results in terms of mass resolution are obtained for microcrystalline surface-preparation protocols. Firstly, surface roughness is much less pronounced, however, the spread in axial velocity resulting from the different orientation of the surfaces of coarse crystals may have an even stronger detrimental effect.

Whereas this explains the relative v_0 differences observable for one matrix, it is clear, however, that the general definition of the v_0 value by the matrix cannot be explained within this frame. It is suggested that the given crystalline and solid state cohesions of the matrix crystals determine the amount of thermal stress, or mechanical energy, respectively, which is accumulated in the crystals until the explosive disintegration into clusters takes place. Indeed, the first practical control for a MALDI preparation is to compare the dried matrix–analyte mixture to the neat matrix, and any change in the microscopic appearance is taken as an indication for problems to be expected. The tolerance against some even high-concentration salt contaminants could be rationalized by a separation upon drying and crystallization. Including the results from Section 4.1, it appears reasonable to assume that this is also the secret of the MALDI softness and the most important parameter to define a matrix, since evaporation is clearly not sufficient to desorb and ionize larger biomolecules and even not small but charged analytes.

4.3. The empirical correlation between matrix softness and a high initial ion velocity

As already pointed out in our first report on the measurements of the initial ion velocity, there exists a qualitative agreement between the softness of the

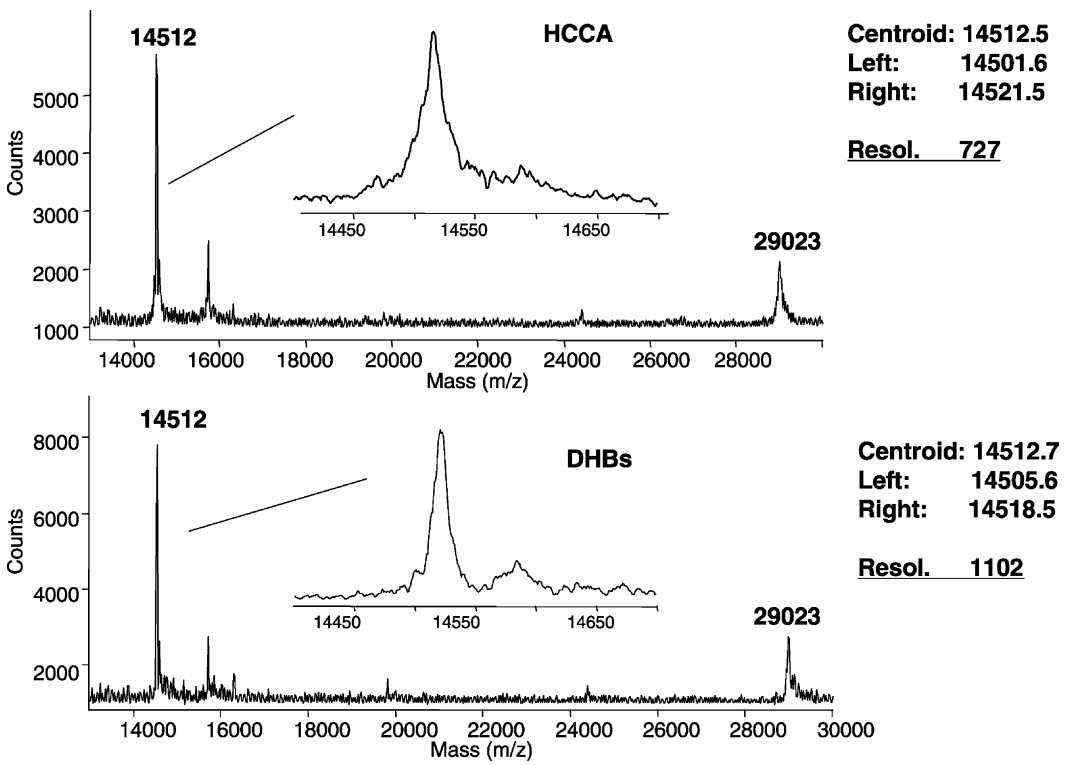

Fig. 2. MALDI mass spectra of carbonic anhydrase obtained with different sample preparation procedures. Upper trace: α-cyano-4-hydroxycinnamic acid (HCCA) using formic acid/water/isopropanol as solvent [27]. Lower trace: mixture of 2,5-dihydoxybenzoic (DHB) acid and 5-methoxy-2-hydroxybenzoic acid (9:1) using TFA (0.1%)/acetonitrile (2:1) as solvent.

matrix and a high v_0 value. Until now, no contradiction to this empirical rule was found. The v_0-increasing effect of some additives was documented in several experiments and agreed, e.g., with the advantages found for DHBs [24,25], i.e., the admixture of 5-methoxy salicylic acid to DHB. Also the first successful application of MALDI in an FTICR mass spectrometry was carried out by admixing a small oligosaccharide, like fructose or ribose [26], and a strong enhancement for v_0 was determined for those crystal layers. 3-Hydroxypicolinic acid is still the only matrix of choice for larger oligonucleotides. By inspecting a 7300 Da DNA again a very high initial velocity is determined: 625, 630 and 601 m/s for the $[MH]^+$, $[MH_2]^{2+}$ and $[MH_3]^{3+}$ ion, respectively. Most interestingly, this high initial velocity is only detected from those spots where an intense emission of molecule ions is possible, whereas a considerably lower initial velocity is recorded for inferior spots.

Another indicative example is the variation of the solvent to formic acid/water/isopropanol (FWI) for the HCCA matrix proposed by Cohen and Chait [27] and recently, Cadene and Chait [28], applied to difficult-to-analyze membrane proteins. This is in strong contrast to the fact that despite the excellent performance of HCCA for the peptide range, which made HCCA the standard matrix in proteomic approaches, intact proteins are rather measured using sinapic acid or DHBs. For carbonic anhydrase as a test analyte, indeed a prominent increase in the initial ion velocity was detected (see Fig. 2, upper spectrum) as compared to water acidified by trifluoroacetic acid/acetonitril solvent mixtures (ATW). The initial ion velocity determined for this preparation using FWI is 420 m/s compared to about 270–290 m/s for a typical dried-droplet or surface HCCA preparation using ATW. This is compared to a DHBs spectrum (lower spectrum) with the typical even higher v_0 value of 550 m/s. As exhibited by the extentions of the doubly-protonated molecular ion signals, tailing to the low-mass side is still less pronounced for DHBs pointing to lower ion excitation and fragmentation for the higher-velocity matrix. This substantiates the assumption that the initial ion velocity can be regarded as a measure for the extent of cluster-jet formation. The faster and the more directed the jet is the better is the entrainment and the expansional cooling of the analyte.

5. Conclusions

In a series of experiments, open questions for a more comprehensive understanding of the fundamental MALDI processes have been addressed. The initial ion velocity is described to be a meaningful tool to differentiate the typical MALDI case of large and typically charged bioanalytes from the intermediate mechanism active for small to medium-size neutral and thermally stable analytes. The high and uniform initial ion velocity for (even low mass) ionic analytes and for all analytes of a molecular size above 3000 Da indicates that they all stem from one source; this is the jet of clusters which results from the ablative explosion of the matrix–analyte crystals once the threshold energy is reached. A true incorporation of the analyte, as clearly obtained for large single crystals, but also in dried-droplet protocols and even assumed for surface protocols, forms the prerequisite for the analyte entrainment and successful analyte-ion generation. A transfer of charged and/or large analytes into the gas phase is not possible by evaporation, presumably either because the required energy density will inevitably result in their destruction or due to insufficient entrainment of large species into a not well-developed gas jet. This further substantiates the cluster ionization (“Lucky-survivor”) model hypothesizing cluster formation and their (partial) charging as the major primary ionization process in MALDI. The initial ion velocity is a matrix property determined by solid state properties. The empirical correlation between high initial velocities and degree of matrix softness attributed to the capacity of a matrix to account for expansional cooling is supported by further examples.

References

[1] P. Juhasz, M.L. Vestal, S.A. Martin, J. Am. Soc. Mass Spectrom. 8 (1997) 209.
[2] M. Glückmann, M. Karas, J. Mass Spectrom. 34 (1999) 467.

[3] R.C. Beavis, B.T. Chait, Chem. Phys. Lett. 181 (1991) 479.
[4] V. Bökelmann, B. Spengler, R. Kaufmann, Eur. Mass Spectrom. 1 (1995) 81.
[5] L.V. Zhigilei, P.B.S. Kodali, B.J. Garrison, Chem. Phys. Lett. 276 (1997) 269.
[6] L.V. Zhigilei, B.J. Garrison, Rapid Commun. Mass Spectrom. 12 (1998) 1273.
[7] M. Karas, M. Glückmann, J. Schäfer, J. Mass Spectrom. 35 (2000) 1.
[8] A. Ingendoh, M. Karas, F. Hillenkamp, U. Giessmannn, Int. J. Mass Spectrom. Ion Process. 131 (1994) 345.
[9] B. Spengler, U. Bahr, M. Karas, F. Hillenkamp, Anal. Instrum. 17 (1&2) (1988) 173.
[10] P. Demirev, A. Westman, C.T. Reimann, P. Håkansson, D. Barofsky, B.U.R. Sundqvist, Y.D. Cheng, W. Seibt, K. Siegbahn, Rapid Commun. Mass Spectrom. 6 (1992) 187.
[11] K. Riahi, G. Bolbach, A. Brunot, F. Breton, M. Spiro, J.-C. Blais, Rapid Commun. Mass Spectrom. 8 (1994) 242.
[12] K. Dreisewerd, M. Schürenberg, M. Karas, F. Hillenkamp, Int. J. Mass Spectrom. Ion Process. 141 (1995) 127.
[13] K. Dreisewerd, M. Schürenberg, M. Karas, F. Hillenkamp, Int. J. Mass Spectrom. Ion Process. 154 (1995) 171.
[14] G.R. Kinsel, M.E. Gimon-Kinsel, K.J. Gillig, D.H. Russell, J. Mass Spectrom. 34 (1999) 684.
[15] B. Spengler, V. Bökelmann, Nucl. Instrum. Meth. B 82 (1993) 379.
[16] T.-W.D. Chan, I. Thomas, A.W. Colburn, P.J. Derrick, Chem. Phys. Lett. 222 (1994) 579.
[17] M. Sadeghi, X. Wu, A. Vertes, J. Phys. Chem. B 105 (2001) 2578.
[18] X. Wu, M. Sadeghi, A. Vertes, J. Phys. Chem. B 102 (1998) 4770.
[19] M. Glückmann, A. Pfenninger, R. Krüger, M. Thierolf, M. Karas, V. Horneffer, F. Hillenkamp, K. Strupat, Int. J. Mass Spectrom. 208 (2001) 121.
[20] A. Pfenninger, M. Karas, B. Stahl, G. Sawatzki, B. Finke, J. Mass Spectrom. 34 (1999) 98.
[21] R. Krüger, A. Pfenninger, I. Fournier, M. Glückmann, M. Karas, Anal. Chem. 73 (2001) 5812.
[22] S. Trimpin, A. Rouhanipour, R. Az, H.J. Räder, K. Müllen, Rapid Commun. Mass Spectrom. 15 (2001) 1364.
[23] W. Zhang, B.T. Chait, Int. J. Mass Spectrom. Ion Process. 160 (1997) 259.
[24] M. Karas, H. Ehring, E. Nordhoff, B. Stahl, K. Strupat, F. Hillenkamp, M. Grehl, B. Krebs, Org. Mass Spectrom. 28 (1993) 1476.
[25] U. Bahr, J. Stahl-Zeng, E. Gleitsmann, M. Karas, J. Mass Spectrom. 32 (1997) 1111.
[26] A. Castoro, C.L. Wilkins, Anal. Chem. 65 (1993) 2621.
[27] S.L. Cohen, B.T. Chait, Anal. Chem. 68 (1996) 31.
[28] M. Cadene, B.T. Chait, Anal. Chem. 72 (2000) 5655.